Available online at www.sciencedirect.com
SCIENCE DIRECT
Biochimica et Biophysica Acta 1708 (2005) 79–90
BIOCHIMICA ET BIOPHYSICA ACTA
BBA
http://www.elsevier.com/locate/bba

Control of cytochrome b_6f at low and high light intensity and cyclic electron transport in leaves

Agu Laisk[a,*], Hillar Eichelmann[a], Vello Oja[a], Richard B. Peterson[b]

[a]*Tartu Ülikooli Molekulaar-ja Rakubioloogia Instituut, Riia tn. 23, Tartu, 51010, Estonia*
[b]*Department of Biochemistry and genetics, The Connecticut Agricultural Experiment Station, 123 Huntington St., New Haven, CT 06511, U.S.A.*

Received 23 August 2004; received in revised form 11 January 2005; accepted 20 January 2005
Available online 18 March 2005

Abstract

The light-dependent control of photosynthetic electron transport from plastoquinol (PQH_2) through the cytochrome b_6f complex (Cyt b_6f) to plastocyanin (PC) and P700 (the donor pigment of Photosystem I, PSI) was investigated in laboratory-grown *Helianthus annuus* L., *Nicotiana tabaccum* L., and naturally-grown *Solidago virgaurea* L., *Betula pendula* Roth, and *Tilia cordata* P. Mill. leaves. Steady-state illumination was interrupted (light–dark transient) or a high-intensity 10 ms light pulse was applied to reduce PQ and oxidise PC and P700 (pulse-dark transient) and the following re-reduction of $P700^+$ and PC^+ was recorded as leaf transmission measured differentially at 810–950 nm. The signal was deconvoluted into PC^+ and $P700^+$ components by oxidative (far-red) titration (V. Oja et al., Photosynth. Res. 78 (2003) 1–15) and the PSI density was determined by reductive titration using single-turnover flashes (V. Oja et al., Biochim. Biophys. Acta 1658 (2004) 225–234). These innovations allowed the definition of the full light response curves of electron transport rate through Cyt b_6f to the PSI donors. A significant down-regulation of Cyt b_6f maximum turnover rate was discovered at low light intensities, which relaxed at medium light intensities, and strengthened again at saturating irradiances. We explain the low-light regulation of Cyt b_6f in terms of inactivation of carbon reduction cycle enzymes which increases flux resistance. Cyclic electron transport around PSI was measured as the difference between PSI electron transport (determined from the light–dark transient) and PSII electron transport determined from chlorophyll fluorescence. Cyclic e^- transport was not detected at limiting light intensities. At saturating light the cyclic electron transport was present in some, but not all, leaves. We explain variations in the magnitude of cyclic electron flow around PSI as resulting from the variable rate of non-photosynthetic ATP-consuming processes in the chloroplast, not as a principle process that corrects imbalances in ATP/NADPH stoichiometry during photosynthesis.

Keywords: Cytochrome b_6f; Control; Leaf

1. Introduction

Electron transport from PSII to PSI is under the tight control of Cyt b_6f [1], which oxidises PQH_2 and transfers e^- to PC while performing the Q-cycle [2,3]. As a result of the latter, the transport of 2 e^- through the Cyt b_6f complex is coupled to the transport of $4H^+$ from the stroma to the thylakoid lumen. The resulting proton-motive force (mainly ΔpH) drives the synthesis of ATP, so that the equilibrium $ATP/(ADP \cdot P_i)$ is positively related to the ΔpH. When photosynthesis is limited by availability of e^- acceptors (e.g. restricted CO_2 supply due to closed stomata), both the ATP/ADP ratio and equilibrium ΔpH increase and exert thermodynamic counter-pressure to H^+ release during the oxidation of PQH_2. As a result, the e^- transport rate through Cyt b_6f complex decreases with increasing counter-pressure of H^+. This phenomenon, termed "photosynthetic control", makes Cyt b_6f the actual rate-limiting step in photosynthesis,

Abbreviations: Chl, chlorophyll; Cyt, cytochrome; e^-, electron(s); FeS, Rieske FeS complex; FRL, far red light; NPQ, non-photochemical quenching of excitation; PC, plastocyanin; PAD, PFD, photon flux density, absorbed and incident; PQ, PQH_2 plastoquinone, oxidised and reduced; PSI, Photosystem I; PSII, Photosystem II; P700, donor pigment of PSI; WL, white light

* Corresponding author. Institute for Molecular and Cell Biology, Tartu University, Riia St. 23 Tartu 51010, Estonia. Tel.: +372 736 6021; fax: +372 742 0286.
E-mail address: alaisk@ut.ee (A. Laisk).

0005-2728/$ - see front matter © 2005 Elsevier B.V. All rights reserved.
doi:10.1016/j.bbabio.2005.01.007

adjusting to downstream limitations such as CO_2 diffusion through stomata or end-product synthesis rate [4,5].

The slow turnover of Cyt b_6f causes the accumulation of oxidised P700 [6]. The turnover rate of Cyt b_6f has been quantified based on the rate of e^- arrival to previously oxidised $P700^+$, measured optically as a transient absorptance change at about 810 nm [7]. The speed of post-illumination $P700^+$ re-reduction varies about 3–4 times depending on the external limitation of photosynthesis [8,9]. Such measurements have so far been carried out only under saturating light, because pre-oxidation of P700 is required for the measurement. Therefore, the control of Cyt b_6f turnover under limiting light has remained unstudied. Early evidence indicating no apparent change of Cyt b_6f turnover in the light-limited range of photosynthesis [7,8] could be ascribed to an interplay between the increasing V_m of Cyt b_6f and the decreasing substrate PQH_2 concentration with decreasing PFD. Furthermore, the 810 nm transmission signal is not a specific indicator of the $P700^+$ level because a similar optical effect is generated by PC^+, which undergoes a redox transient that is not proportional to $P700^+$ [10,11]. The post-illumination re-reduction transient observed using the raw 810 nm signal is a coincidental, nearly exponential overlapping of the two signals. As a result, the reported exponential time constants are not quantitative, but only apparent indicators of $P700^+$ re-reduction speed.

In this work we revisited the problem of regulation of Cyt b_6f turnover during photosynthesis using contemporary techniques for determining PSI density and 810 nm signal deconvolution. We reductively titrated the amount of P700 in leaves, generating e^- from PSII with a single turnover flash and measuring the optical effect when they arrived at PSI [12]. We also applied the 810 nm signal deconvolution algorithm, which allowed us to calculate the actual speed of e^- arrival at the high-potential donors of PSI [13]. In order to induce P700 oxidation under low light, we applied strong, yet brief, saturation pulses to oxidise P700 but avoid inducing changes in the control of Cyt b_6f turnover [14]. These innovations revealed that the control of Cyt b_6f turnover is active not only in the light-saturated range of photosynthesis, but also during light-limitation. The successful quantification of e^- transport rates through PSII and PSI showed that cyclic e^- transport, calculated as the difference between PSI and PSII rates, was under the threshold of detection in some leaves, but present in others. This approach also allowed us to compare non-photochemical quenching of PSII excitation and photosynthetic control of Cyt b_6f turnover, both of which are believed to be ΔpH-controlled.

2. Materials and methods

2.1. Plant material

Sunflower (*Helianthus annuus* L.) and tobacco (*Nicotiana tabaccum* L.), wild type, Cyt b_6f deficient transgenic [15] and Rubisco deficient transgenic [16] plants were grown hydrponically under 'high light' PFD of 600–800, and 'low light' PFD of 40–60 μmol quanta m^{-2} s^{-1}, a 12/12 h day/night length and a temperature of 25/20 °C day/night. Full-grown leaves attached to the plant were used in the measurements. Plants of *Solidago virgaurea* L. and shoots of *Betula pendula* Roth and *Tilia cordata* P. Mill. were collected from the opposite ends of their occurrence along the natural gradient of irradiance in a mixed deciduous forest stand in Järvselja, Estonia, 58°22′N, 27°20′E, and transported to the laboratory [17].

2.2. Gas exchange measurements

The properties of the two-channel fast-response measurement system (Fast-Est, Tartu, Estonia) have been described [13,14,18]. A part of a leaf was enclosed in a sandwich-type chamber (diameter=31 mm, height=3 mm) and flushed with gas at a rate of 0.5 mmol s^{-1}. Leaf temperature was stabilised at 22 °C and the water vapour pressure deficit of the flushing gas was maintained at 1.7 kPa. Leaf transpiration was recorded by use of a micro-psychrometer (Fast-Est, Tartu, Estonia), enabling the calculation of the stomatal conductance of the leaf. Desired O_2 and CO_2 concentrations were generated by mixing pure cylinder gases at controlled flow rates. Net CO_2 uptake by the leaf was measured with a LI-6251 infrared gas analyser (LiCor, Lincoln, NE, USA). Oxygen evolution from the leaf after a single turnover flash was measured in the same flow-through system with a Zr–oxide O_2 analyser Ametek S-3A (Thermox, Pittsburgh, PA). For measurements of O_2 evolution the background O_2 concentration was temporarily decreased to 30–100 μmol mol^{-1} for no longer than 10 min.

The leaf chamber was illuminated through a multi-arm plastic fibre-optic light guide (Fast-Est, Tartu, Estonia). Two Schott KL 1500 (from H. Walz GmbH, Effeltrich, Germany) tungsten halogen light sources equipped with necessary filters provided actinic illumination (WL) and saturation pulses of 10 000 μmol quanta m^{-2} s^{-1} (duration 1.4 to 2.5 s, dependent on actinic light for F_m measurements, and 10 ms for P700 oxidation). Computer-operated electro-pneumatic shutters (Fast-Est, Tartu, Estonia) were installed in the KL 1500 sources to open and close the WL and saturation beams with full pulse edges of 1.3 ms. Single-turnover flashes (up to 60 μmol quanta m^{-2} from a Xe-lamp source, 4 μs) were produced by a Machine Vision Strobe MVS-7060 (EG&G Optoelectronics, Salem, MA). Far-red light centred at 720 nm (FRL) was provided with a KL 1500 incandescent source equipped with an interference filter from Andover, Salem, NH, USA. The incident WL (400–700 nm) was measured by a LI-190SB quantum sensor (LiCor, Lincoln, NE). The spectral distribution of the WL and FRL sources and the absorption coefficient of the leaf were measured in a home-made integrating sphere using spectro-radiometer PC-2000 (Ocean Optics, Dunedin, FL) and the absorbed photon fluence rates of WL and FRL were computed from the

spectral distributions of the light source and leaf absorptance [13]. PSI excitation rate, k_{Iq} (s^{-1}), was calculated considering the relative optical cross-section of PSI, a_I:

$$k_{Iq} = a_I I / N_I \quad (1)$$

where I is the absorbed quantum fluence rate (PAD, μmol quanta m^{-2} s^{-1}) and N_I is the PSI density (μmol m^{-2}) determined as described below.

2.3. Relative optical cross-sections of PSII and PSI antennae

The quantum yield of linear e^- transport supporting CO_2 reduction and photorespiration was measured at limiting PFDs and the same e^- flow rate was assumed to pass through PSII and PSI (cyclic and pseudo-cyclic e^- transport were neglected at low PFDs). Fluorescence-indicated losses of quanta in PSII, and losses in PSI due to acceptor side closure (indicated by pulse-oxidation of P700) were considered, enabling the calculation of the fractions (a_{II} and a_I) of the total absorbed quanta absorbed by PSII and PSI, respectively [14,19,20].

2.4. Chlorophyll fluorescence and PSII electron transport

Chl fluorescence was measured using fibres covering an ellipsoid of 1×2 cm^2 individually arranged between the illumination fibres. The fibres were connected to a ED-101 emitter-detector unit of a PAM 101 fluorometer (H Walz, Effeltrich, Germany). Fluorescence readings were corrected for the cross-sensitivity of the detector to the emitter light, saturation of the detector at high actinic PFDs, under-saturation of the F_m pulse, and for PSI fluorescence [21]. The PSII electron transport rate was calculated from fluorescence according to [22], considering the actual optical cross-section of PSII, a_{II}. PSI reduction rate by e^- coming from PSII, k_{IF}, was calculated considering the e^- flow rate and PSI density, N_I, determined from reductive titration (below):

$$k_{IF} = a_{II} I \frac{F_m - F_s}{F_m} \frac{1}{N_I}, \quad (2)$$

where I is the absorbed photon fluence rate, F_s is the steady-state and F_m the pulse-saturated fluorescence yield in the light.

Non-photochemical quenching of excitation (NPQ) is presented as the rate constant of H^+-dependent thermal decay, calculated relative to the basic physically determined rate constant [23,24]:

$$NPQ = \frac{F_{md}}{F_m} - 1, \quad (3)$$

where F_m is the pulse-saturated fluorescence yield in the light-adapted state and F_{md} is the fully dark-adapted (predawn) maximum fluorescence yield.

2.5. Differential leaf transmittance at 810–950 nm and P700DW signal conversion

A bundle of fibres illuminating a 1 cm^2 area in the centre of the top side of the leaf was connected to the emitter of a modified dual-wavelength ED P700DW emitter-detector module operating at 810 and 950 nm (H. Walz, Effeltrich, Germany). A similar bundle on the rear side of the chamber delivered transmitted measuring light to the detector. The raw recorded signal from this device is termed 'P700DW signal' below.

The P700DW signal, calibrated for full reduction in the dark and full oxidation during a saturation pulse applied on a background of FRL, was deconvoluted into PC^+ and $P700^+$ components and presented as e^- per PSI in the high-potential donors using the oxidative (far-red) titration method [13]. The dark-reduced PSI donor side was re-oxidised under FRL and the P700DW signal transient was modelled assuming redox equilibrium between the PSI donor side carriers Cyt *f*, PC and P700 (equilibrium constants 25 between P700 and PC, and 63 between P700 and Cyt *f*, optical effect of one e^- in P700 was considered to be 5 times greater than in PC). Best-fit relative pool sizes (FeS+Cyt *f*)/P700 and PC/P700 were inferred from the model. A mathematical algorithm was derived from the model to convert the P700DW signal into the relative number of e^- in these carriers per PSI.

2.6. Determination of PSI density

The reductive titration of PSI by the e^- generated in PSII was used to determine the absolute PSI density [12]. The donor side of PSI was oxidised under FRL. A saturating single turnover flash was applied and the FRL was turned off simultaneously. The number of e^- generated from PSII was calculated as 4 times integrated O_2 evolution [25]. The change in the P700DW signal was recorded as these electrons arrived at PSI. The P700DW signal was deconvoluted into $P700^+$ and PC^+ components and the number of e^- necessary for the full reduction of previously oxidised P700 was found. This value represented the PSI density.

2.7. Operation of the system and data recording

The system was operated and data were recorded using an A/D converter board ADIO 1600 (ICS Advent, San Diego, CA) and a system-operation and data-recording program RECO (Fast-Est, Tartu, Estonia). A textual meta-language script composed using a word processor executed Turbo Pascal routines that in turn operated gas mixers, light sources, and shutters in pre-programmed experiments.

2.8. Standard experimental routine

Stomatal opening was induced under PFD of 720 μmol quanta m^{-2} s^{-1} and the light response of photosynthesis

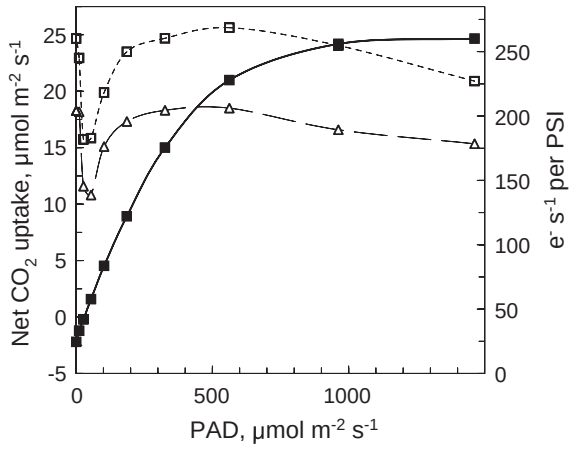

Fig. 1. Light response curve of net CO_2 uptake of a high light-grown sunflower leaf (filled squares and thick line) and of the rate of pulse-dark e^- arrival at PSI (open squares and dotted line, right ordinate). For comparison, the post-pulse raw P700DW signal transient was approximated by an exponential function and the reciprocal of the time constant ($1/\tau$, right ordinate) is shown as a function of PAD (empty triangles and dashed line). Incident photon flux density (PFD) was applied in the following order: 2000, 1310, 760, 438, 249, 138, 73, 35, 13, and 0 μmol quanta m^{-2} s^{-1}, 5 min exposure, CO_2 concentration 0.036%, O_2 concentration 21%, leaf temperature 22–23 °C.

was measured by decreasing the PFD stepwise from 2000 to 0 μmol quanta m^{-2} s^{-1}. The flushing gas contained 21% O_2 and 0.036% CO_2 (balance N_2) and the leaf temperature was 22 to 23 °C (Fig. 1). The exposure at each light level lasted 5 min. At the end of each exposure, the post-pulse P700DW signal transient was measured by applying a 10 ms saturation pulse and then shuttering all light off for 100 ms. The measurement was repeated 5 times after a 10 s stabilisation time, and the transients were averaged. After a 10 s relaxation time, the post-illumination P700DW transient was measured by shuttering the light off for 100 ms without the saturation pulse, also repeated 5 times (this procedure was omitted at limiting PFDs since the oxidation of the PSI donor side was very low and no "re-reduction" could be recorded). After an additional 10 s, the Chl fluorescence measuring beam was turned on and the F_s and F_m values were recorded, after which the actinic light was decreased to the next step in the sequence. The millisecond-length pulsing and darkening did not disturb steady-state photosynthesis. The oxidative and reductive titrations of PSI were carried out on the same leaf before measurement of the light response curve.

The data are presented as e^- arrival rate at PSI or excitation rate of PSI, in e^- per PSI s^{-1} or quanta per PSI s^{-1}. The following system of denotations is used. The e^- arrival rate at PSI (e^-s^{-1}) is denoted k_I (subscript I indicates PSI). A similar rate, but related to Cyt b_6f, is denoted k_C. The second subscript at k_{Im} and k_{Cm} denotes the maximum, substrate-saturated rate, analogous to V_m of an enzyme-catalysed reaction. The rate of PSII e^- transport, calculated from fluorescence, but related to PSI, is denoted k_{IF}, while the rate of PSI excitation by absorbed quanta is denoted k_{Iq}.

3. Results

3.1. Post-illumination and post-pulse re-reduction of PSI e^- donors

Post-illumination and post-pulse P700DW signal transients were deconvoluted into $P700^+$ and PC^+ components using the oxidative (far-red) titration method and transformed into the number of e^- per PSI in the donor side carriers (Cyt *f*+FeS)+PC+P700 (Fig. 2). The initial slope of the deconvoluted light–dark (or pulse-dark) transient represents the e^- transport rate to PSI, in e^-s^{-1} per PSI (actually, the maximum slope of the pulse-dark transient was used because the decreasing ferredoxin signal seemed to interfere with the $P700^+$ and PC^+ signals at the beginning of the transient). The pulse-dark rate corresponded to the maximum rate (V_m) of Cyt b_6f turnover, because the pulse reduced the PQ pool and oxidised the donor side of PSI. As explained above, we denote this rate as k_{Im}, because it depends not only on the rate of Cyt b_6f turnover, but also on the ratio of active Cyt b_6f and PSI per leaf area,

$$k_{Im} = k_{Cm}N_C/N_I \quad (4)$$

where k_{Cm} is the maximum rate of Cyt b_6f turnover and N_C and N_I are the area densities of photosynthetically active Cyt b_6f and PSI complexes. Measurement of the actual steady-

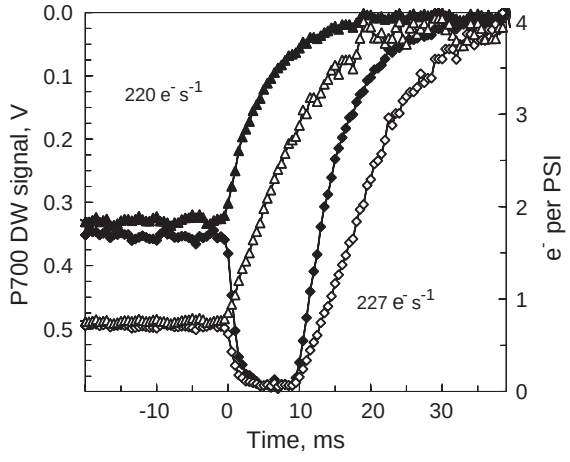

Fig. 2. Measurement of light–dark (triangles) and pulse-dark (diamonds) transients and the transformation of the raw P700DW signal (filled symbols, left ordinate) into the number of e^- per PSI (open symbols, right ordinate) in the high-potential donors in a high light-grown sunflower leaf. At time=0 either steady-state illumination was interrupted (triangles) or a 10 ms saturation pulse was applied and thereafter the leaf was darkened. The rate of e^- arrival at PSI is presented by the initial (or maximum, see text) slope of the transient. Steady-state PAD was 1520 μmol quanta m^{-2} s^{-1}; values of light–dark and pulse-dark e^- arrival rates at PSI were 220 and 227 s^{-1}, respectively. The recordings are averages of 5 traces.

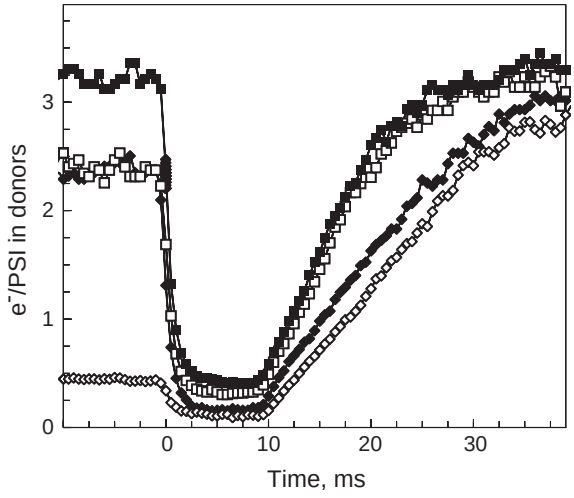

Fig. 3. Pulse-dark re-reduction of PSI donors in a sunflower leaf. The pulse was applied at steady-state PAD of 1520 (empty diamonds), 342 (empty squares), 28 (filled diamonds) and 0 μmol quanta m^{-2} s^{-1} (filled squares) and the respective e^- arrival rates were 118, 213, 128 and 214 e^-s^{-1} per PSI. In this leaf the e^- capacity of the PSI high-potential donors was 3.2 e^-/PSI, distributed as 1 e^- in P700, 1.4 e^- in PC and 0.8 e^- in Cyt *f* in the fully reduced state.

state rate k_I from the light–dark transient was possible only at nearly and fully saturating PFDs, when the PSI donor side became sufficiently oxidised. Under partial light limitation k_I was slower than k_{Im}, but approached k_{Im} at full light saturation.

Fig. 3 illustrates how k_{Im} is measured at different PFDs in a sunflower leaf. The level of the deconvoluted signal before the pulse presents the number of e^- in PSI donors during steady-state illumination. In the dark the donors were reduced and the sum of e^- amounted to 3.2 per PSI, shared as 1 in P700, 1.4 in PC and 0.8 in Cyt *f*. Under low and medium PFDs Cyt *f* became about one-half, and PC about one-third, oxidised accounting for 2.4 e^-/PSI. Under the high PFD only 0.45 e^-/PSI remained, almost completely in P700. The 10 ms saturation pulse induced more oxidation of PSI donors compared to the steady-state, but P700 never was completely oxidised (complete oxidation was achieved only when the saturation pulse was superimposed on FRL, denoted as the zero ordinate in Fig. 3). The residual reduction level during the pulse was higher in the dark and became lower with increasing steady-state PFD. After the pulse and the actinic light were shuttered off simultaneously, e^- continued to flow, reducing the oxidised high-potential PSI donors. The rate of e^- arrival (the slope of the deconvoluted curve) was far from exponential, remaining remarkably constant up to about 2.5 e^- transported per PSI, i.e., until $P700^+$ and most of PC^+ became reduced, and the rate decreased only when Cyt *f* became reduced. This initial e^- arrival rate, however, was different when the leaf was pre-exposed in the dark or under different PADs. The rate was fast after the dark exposure, slow at PAD of 28, faster at a moderate PAD of 342 and slow again in the maximum PAD of 1520 μmol quanta m^{-2} s^{-1}. The full light response curve of k_{Im}, along with the photosynthetic CO_2 uptake rate, is given in Fig. 1 for another sunflower leaf. For comparison, we fitted the P700DW signal to a single exponential and presented the reciprocal of the time constant $1/\tau$. This apparently exponential P700 re-reduction rate is by about 30% slower than the true rate, but undergoes changes that parallel k_{Im}.

3.2. Actual and maximum electron transport rate through Cyt b_6f

Although Fig. 1 shows that k_{Im} changes significantly during light-limited photosynthesis, it is not a convenient basis for analysis of Cyt b_6f control because k_{Im} is presented in units of e^-s^{-1} per PSI while the rate of photosynthesis is presented in μmol CO_2 m^{-2} s^{-1}. In a more consistent presentation (Fig. 4), e^- transport rate through PSII during steady-state photosynthesis, calculated from Chl fluores-

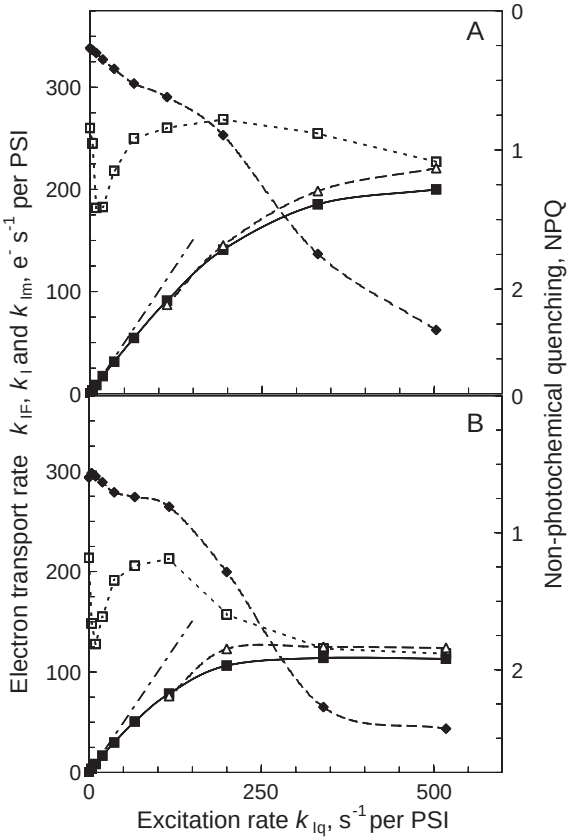

Fig. 4. Electron arrival rate at PSI as a function of PSI excitation rate, k_{Iq}. The steady-state arrival rate k_{IF} of PSII e^- was determined from PSII fluorescence (Eq. (2), filled squares, continuous line), the steady-state e^- arrival rate to PSI through Cyt b_6f, k_I, was determined from the light–dark re-reduction of PSI donors (empty triangles and dashed line) and the maximum, substrate-saturated e^- arrival rate, k_{Im}, was determined from the pulse-dark re-reduction of PSI donors (empty squares and dotted line). The dash-dotted line shows the quantum yield of PSI=1. Diamonds and the right ordinate present non-photochemical quenching NPQ (Eq. (3)). The plant was a high light-grown (panel A) or a low light grown (panel B) sunflower. Data points correspond to incident PFDs given in the legend to Fig. 1.

cence measurements, is presented as $e^{-}s^{-1}$ per PSI, k_{IF} (Eq. (2)), instead of CO_2 uptake. In this presentation the e^{-} transport rate through PSII (k_{IF}), e^{-} transport rate through PSI (k_I, determined from the light–dark transient), and maximum rate through Cyt b_6f (k_{Im}, determined from the pulse-dark transient) are all scaled as $e^{-}s^{-1}$ per PSI. In order to present the abscissa in consistent units, the PAD exciting PSI (μmol quanta m^{-2} s^{-1}) was also divided by PSI density (μmol m^{-2}) resulting in the PSI excitation rate, k_{Iq} (quanta s^{-1} per PSI, Eq. (1)). This unified approach was employed in Figs. 4–7 to characterise typical Cyt b_6f control situations in different species and growth conditions, and also in some transgenic plants.

Sunflower represents a typical C_3 plant with relatively high photosynthetic rate (Fig. 4). Since it had a high PSI density at both growth PFDs, the maximum PSI excitation rate, k_{Iq}, was only about 500 s^{-1} at the maximum incident PFD of 2000 μmol m^{-2} s^{-1}. The steady-state PSII e^{-} transport rate k_{IF} increased in proportion to light intensity and saturated at a level of 200 s^{-1} per PSI in the high light-grown leaf, but at a lower rate of 120 s^{-1} in the low light-grown leaf. The initial slope of the light response curve was close to 1 $e^{-}s^{-1}$ per 1 photon s^{-1} (dash-dotted lines in Figs. 4–7). Since the ordinate depends on the relative optical cross-section of PSII, a_{II} (Eq. (2)), and the abscissa depends on the relative optical cross-section of PSI, a_I (Eq. (1)), an initial slope close to unity indicates that these cross-sections were derived correctly.

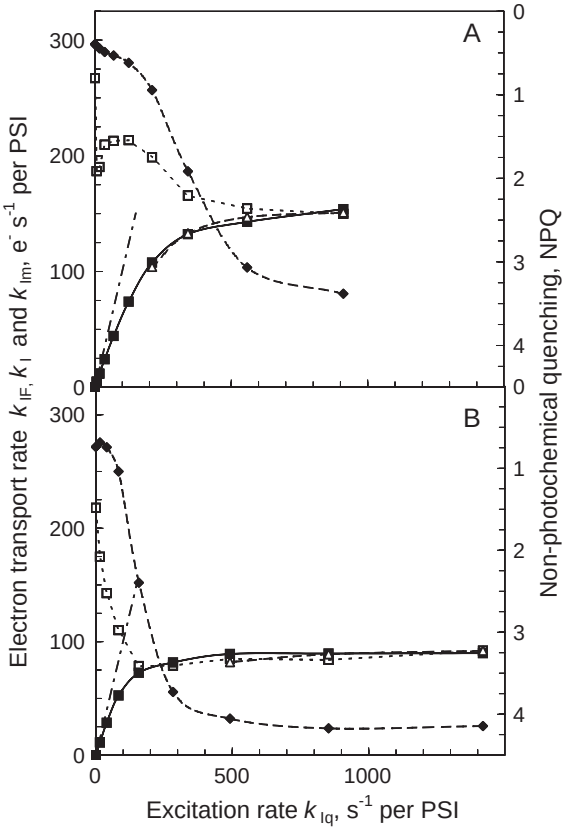

Fig. 5. The same as in Fig. 4, but the plant was naturally growing *S. virgaurea*, collected from a sunny (panel A) or a shaded (panel B) habitat.

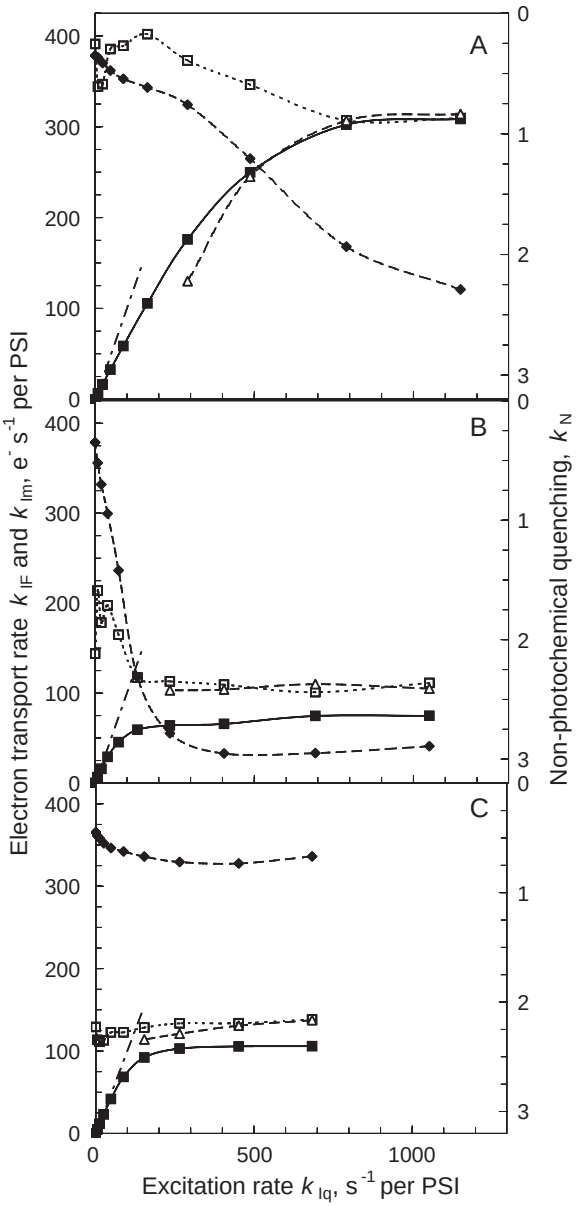

Fig. 6. The same as in Fig. 4, but the plant was laboratory grown tobacco, wild type (panel A), Rubisco deficient transgenic (panel B) and Rieske FeS deficient transgenic (panel C).

The pulse-induced maximum rate of e^{-} arrival at PSI, k_{Im}, was 260 s^{-1} in the dark state in the high light-grown leaf. This dark value best characterises the maximum rate of Cyt b_6f, however this quantity tended to decrease with increasing dark exposure. In the presence of light the pulse-dark re-reduction kinetics was stable and repeatable. Unexpectedly, considerable down-regulation of Cyt b_6f was observed in this and other leaves at very low PFDs of 30–50 μmol quanta m^{-2} s^{-1} (Fig. 4). This down-regulation was reversed at moderate PFDs (PSI excitation rates k_{Iq} of 100–200 s^{-1}), before the onset of light saturation of photosynthesis. Photosynthetic control became significant

again with the onset of light saturation of photosynthesis when the actual rate of e^- transport, k_{IF}, and the maximum rate of Cyt b_6f, k_{Im}, became similar. The control of light-saturated photosynthesis by the turnover of Cyt b_6f was very strong in leaves that had relatively low photosynthetic rates, like low light-grown sunflower (Fig. 4B) and naturally growing *S. virgaurea* (Fig. 5).

Due to the low PSI density in *S. virgaurea* the PSI excitation rate exceeded 1000 s^{-1} at an incident PFD of 2000 μmol quanta m^{-2} s^{-1}. Despite the lower PSI density, the basic dark-relaxed k_{Im} was still 250 to 270 s^{-1} and it rapidly decreased to 180 s^{-1} under low light, as in sunflower. In the high light-grown *S. virgaurea* (Fig. 5A) the Cyt b_6f control relaxed to 220 s^{-1} at medium PFDs, while in the shade-grown plant (Fig. 5B) the carbon reduction-limited electron transport rate was so slow that the control did not relax, but remained strong over the entire PFD range. In shade-grown *S. virgaurea* at light saturation, Cyt b_6f was down-regulated to about 1/3 of its dark rate.

Wild-type tobacco was remarkable in terms of its very high k_{Im} of up to 400 s^{-1} in the dark state (Fig. 6A). Still, it was not an intrinsic property of Cyt b_6f of this plant, but rather, was caused by the relatively low PSI density compared to the Cyt b_6f density (Eq. (4)). In other aspects, wild-type tobacco behaved like sunflower, except that the low-light depression of k_{Im} was somewhat smaller.

The Rubisco-deficient transgenic tobacco was chosen to represent a plant with severely limited CO_2 uptake rate due to artificially unbalanced development of the photosynthetic machinery. Interestingly, it exhibited a new feature: At light saturation the e^- transport rate through PSI, k_I, measured as light–dark re-reduction rate, was faster than the e^- transport rate through PSI calculated from fluorescence measurements (Fig. 6B). This difference disappeared when measurements were carried out at saturating CO_2 concentrations (not shown). Another interesting plant for the investigation of e^- transport through Cyt b_6f was the Cyt b_6f deficient transgenic tobacco. In this plant the basic, dark-state e^- transport rate, k_{Im}, was slow (120 s^{-1}). The rate was very slightly down-regulated at low PFDs and remained practically constant over the whole light response curve (Fig. 6C). The steady-state PSI e^- transport rate was significantly faster than the PSII e^- transport rate.

3.3. Oxygen dependence of the low-light Cyt b_6f control

Atmospheric oxygen concentration is expected to release the photosynthetic control because electron transport is faster due to photorespiration and Mehler reaction than at low O_2 concentrations. Birch leaves collected from the top layer of the canopy behaved in accordance with this notion (Fig. 7). The fluorescence-based e^- transport rate, k_{IF}, was faster under the air level of O_2 than in 2% O_2, correspondingly, at light saturation k_{Im} was down-regulated more in 2 than in 21% O_2. However, the low-light down-regulation of

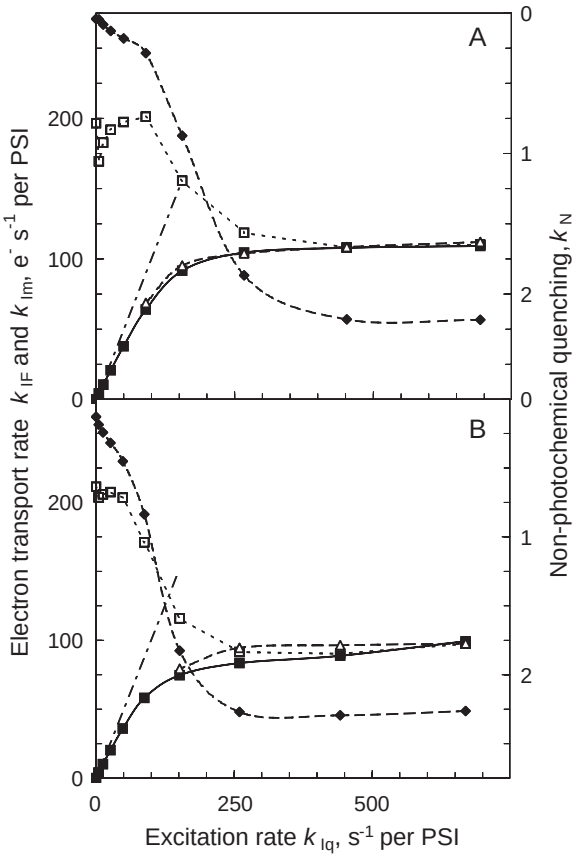

Fig. 7. The same as in Fig. 4, but the plant was high light grown birch measured in the presence of 21 (panel A) and 2% O_2 (panel B).

k_{Im}, present in 21% O_2, was almost absent in 2% O_2. The dependence of the low-light down-regulation of Cyt b_6f on O_2 concentration was confirmed in 64 repeated experiments on birch leaves, such that a relative low-light down-regulation of the V_m of Cyt b_6f (medium light relaxed value minus low-light value divided by the relaxed value) of 12.6±0.6% in 21% O_2 and 2.2±0.3% in 2% O_2 was observed.

3.4. Cyclic electron transport

The actual steady-state e^- transport rate was calculated for PSII from Chl fluorescence and for PSI from the light–dark P700DW signal transient. The latter measurement was possible only at near-saturating and saturating PFDs, where PSI donor side carriers were sufficiently pre-oxidised in the light. The difference (PSI–PSII) between the two e^- transport rates was interpreted as cyclic e^- transport rate around PSI. At nearly limiting PFDs the two e^- transport rates were equal in all plants. In sunflower, at saturating PFDs, the PSI e^- transport rate was about 10% faster than PSII e^- transport, but in other non-transformed plants the difference between the PSI and PSII e^- transport rates was not significant either at limiting or saturating PFDs. In both of the transgenic tobacco plants cyclic e^- transport occurred at about 25–50% of the linear (PSII) rate.

Table 1 summarises the data for the plants studied. Here we present the maximum turnover rate for Cyt b_6f, k_{Cm} (Eq. (4)), calculated on the basis of the relative abundance of Cyt f and PSI (n_C=N_C/N_I), as revealed from the oxidative titration of PSI donors. Though the method determines n_C relatively unreliably, the calculation of average values of k_{Cm} could reveal differences between species. The basic features observed in individual leaves–down-regulation of k_{Cm} at low PFDs, relaxation at moderate PFDs and down-regulation again at light saturation–are present also in the averaged data. In leaves with high photosynthetic rate the medium-light k_{Cm} may exceed the low-light minimum by 15 to 25%. Conversely, in low-light grown leaves with low photosynthetic rate (*T. cordata* and *S. virgaurea*) e^- transport is so restricted that medium-light relaxation is not observed. The dark-relaxed k_{Cm} seems to be variable among species. In transgenic leaves (Table 1) the individual variations of k_{Cm} were so extreme as to preclude meaningful comparisons of this average to those of other species and conditions.

3.5. Relationship between non-photochemical quenching and photosynthetic control

Both e^- transport through Cyt b_6f and non-photochemical quenching of PSII excitation (NPQ, Eq. (3)) are believed to be controlled by lumenal pH. The light dependence of NPQ was plotted in Figs. 4–7 for comparison with k_{Im}. When light became saturating both parameters changed in parallel, as expected, but little increase in NPQ was observed in parallel with the relatively strong down-regulation of k_{Im} at low PFDs. Such complex interdependence is illustrated by Fig. 8, which relates NPQ to k_{Cm} using data from Figs. 4–6. The use of k_{Cm} instead of k_{Im} minimises variations between leaves caused by different Cyt b_6f/PSI ratios, but may introduce a random component of variability, because of methodological uncertainty in determination of Cyt f density. At saturating PFDs k_{Cm} and NPQ are related like pH-dependent processes possessing different pK values [pK (k_{Cm})>pK (NPQ)]. Specifically, k_{Cm} falls faster initially while NPQ is still slowly increasing, and k_{Cm} is approaching the minimum when NPQ is still rapidly increasing. However, effectors other than pH appear to be operating since the range of k_{Cm} variation seems to vary.

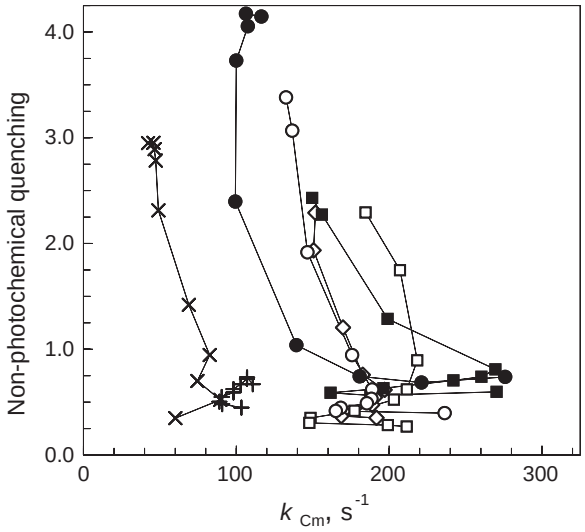

Fig. 8. Relationships between non-photochemical quenching, NPQ, and maximum turnover rate of Cyt b_6f, k_{Cm}, in individual leaves of sunflower (squares), *S virgaurea* (circles), wild type tobacco (diamonds), Rubisco-deficient tobacco (diagonal crosses) and Rieske FeS deficient tobacco (horizontal crosses). Empty symbols, high growth light; filled symbols, low growth light.

Table 1
Photosynthetic parameters and light-dependent regulation of cytochrome b_6f turnover in different plants (±S.E. n=4 to 8)

		N_{II}	N_I	n_{PC}	n_{cyt}	k_{Cm} (s^{-1})				J_{cyc} (%)
		μmol m^{-2}		Per PSI		Dark	Min	Relax	Sat. light	
B. pendula	HL	1.33±0.07	1.22±0.07	1.87±0.05	0.95±0.06	208±9	183±8	215±11	131±12	4.9±3.7
	LL	0.96±0.04	0.77±0.04	1.92±0.02	0.83±0.03	222±11	192±13	203±10	120±5	1.4±2.9
T. cordata	HL	1.08±0.16	0.70±0.16	1.99±0.12	1.14±0.04	158±8	149±9	155±6	94±3	−5.5±3.5
	LL	0.97±0.11	0.53±0.11	1.73±0.16	1.00±0.02	198±9	126±12	126±12	71±8	12.2±2.7
S. virgaurea	HL	0.94±0.16	0.74±0.16	1.57±0.15	0.94±0.10	237±11	189±13	203±12	125±4	0.6±3.1
	LL	0.62±0.08	0.37±0.08	1.86±0.11	0.72±0.04	350±17	193±19	193±19	96±10	−1.4±4.1
H. annuus	HL	1.43±0.04	1.03±0.04	1.57±0.27	0.95±0.13	268±42	213±35	285±38	241±26	7.5±4.7
	LL	0.89±0.09	1.03±0.09	1.83±0.15	0.92±0.09	248±26	201±29	240±28	163±25	9.1±2.3
N. tabaccum	HL	0.87±0.07	0.52±0.07	2.19±0.11	1.59±0.06	214±13	197±11	237±7	192±6	−2.1±1.6
	LL	0.39±0.05	0.25±0.05	1.87±0.34	1.30±0.22	203±31	170±24	216±29	165±28	4.5±2.3
RBC deficient		0.16…1.15	0.14…0.91	1.61…4.13	0.86…2.94	53…214	0.93±0.03	1.02±0.06	0.54±0.03	3.1…69.4
Cyt deficient	HL	0.58…1.35	0.38…0.93	2.19…4.34	1.03…2.80	35…104	0.93±0.02	1.00±0.03	0.94±0.03	−2.6…163
	LL	1.22±0.05	0.97±0.05	2.00±0.05	0.77±0.04	136±14	112±11	139±11	132±17	16.7±7.5

HL and LL, high and low growth light; N_{II} and N_I, area densities of PSII and PSI; n_{PC} and n_{Cyt}, relative abundance of plastocyanin and cytochrome f per PSI; k_{Cm}, maximum turnover rate of cytochrome b_6f (in columns from the left to right) in the dark, minimum at low light, relaxed at medium light and down-regulated at light saturation. In transgenic tobacco, where k_{Cm} varied widely, these values are not averaged but the control range is given relative to the dark value in each individual leaf (range indicated with triple dots). J_{cyc} is the cyclic electron transport rate, given as % from the linear (PSII) rate.

4. Discussion

We applied new methods for the assessment of e^- transport rate to the donor side of PSI in leaves. First, we deconvoluted the P700DW signal into the components of $P700^+$ and PC^+ and calculated the rate of e^- arrival at the high-potential PSI donors, k_I, as e^-s^{-1} per P700 [12,13]. Second, we applied the pulse-oxidation of PSI donors in order to measure the re-reduction rate at low PFDs, where the PSI donors are not pre-oxidised by actinic light [14,26].

4.1. Limitation of electron transport by PQ diffusion or Cyt b_6f turnover

The total density of PSII, Cyt b_6f and PSI protein complexes in grana-stacked thylakoid membranes is close to the percolation threshold, where small closed domains are formed, inside which PQ diffusion is fast, but severely restricted over longer distances [27–29]. In those domains where PSII and Cyt b_6f both are present, PQ diffusion from PSII to Cyt b_6f is not rate-limiting. But PQ diffusion may become limiting if one e^- transport partner is absent from the domain and interdomain migration is necessary. A random distribution of PSII and Cyt b_6f should result in the formation of a significant fraction of domains containing only one e^- transport partner, resulting in inhomogeneous, mixed diffusional-kinetic limitation of overall e^- transport. Experimental evidence exists, however, that argues against significant inhomogeneity. When a single-turnover flash is superimposed on FRL, the re-reduction of $P700^+$ begins after a delay of about 1–2 ms [12,30], indicating rapid e^- movement from PSII to PSI which includes the diffusion times of PQ and PC. Though this short delay may reflect the situation in that fraction of domains with favourable diffusion conditions, the constant rate at which $P700^+$ and PC^+ are re-reduced after an oxidising saturation pulse (Figs. 2 and 3) is inconsistent with substantial inhomogeneities in e^- transfer processes. Thus, domains containing both PSII and Cyt b_6f that interact directly [28] are in majority, or the protein density in thylakoids is below the percolation threshold, minimising the diffusional limitation of interphotosystem e^- transport and restricting the site of the rate-controlling step to Cyt b_6f.

4.2. Kinetics of e^- transport through Cyt b_6f

The P700DW signal deconvolution (Figs. 2 and 3) revealed that, when PQ was pre-reduced by the saturation pulse, the rate of e^- arrival at PSI donors was constant while $P700^+$ and PC^+ were being reduced, but decreased when Cyt f was being reduced. This result implies that Cyt b_6f was strongly saturated with respect to plastoquinol. Since the deconvolution of the P700DW signal was based on the assumption of equilibrium between the PSI high-potential donors [13], the logically expected deconvolution result indirectly supports the assumption. The equilibrium concept [31] is also supported by the very fast oxidation of Cyt f after a single-turnover flash in leaf disks (about 5000 s^{-1}), showing the e^- vacancy is very rapidly transferred from P700 to Cyt f, and the very slow re-reduction of Cyt f in the dark, showing that e^- arriving at Cyt f are rapidly forwarded to PC [30].

In previous works the whole post-illumination transient of the 820 nm signal was approximated by an exponent, assumed to reflect $P700^+$ re-reduction [7–9,32,33]. This exponent is only apparent, created by overlapping PC^+ and $P700^+$ signals, and the associated time constant is about 30% longer than the true time of $P700^+$ re-reduction (Fig. 1). Changes in the apparent exponential rate constant, $1/\tau$, paralleled changes in the true k_I (Fig. 1), validating earlier conclusions concerning relative changes in Cyt b_6f turnover rate due to photosynthetic control. But conclusions based on the reduction state of P700 are not supported since this quantity is actually much higher than revealed from the raw 820 nm signal.

4.3. Photosynthetic control of Cyt b_6f turnover in high and low light

The maximum turnover rate (V_m) of Cyt b_6f was near its maximum in the dark, as expected considering that both e^- and H^+ backpressure were minimal. As expected, V_m decreased at light saturation of photosynthesis. However, an unexpected significant down-regulation of the V_m of Cyt b_6f was observed at low PFDs, which relaxed at moderate PFDs. Though the down-regulation of the V_m of Cyt b_6f at saturating light is well known [7–9,26], this low-light control of Cyt b_6f remained undiscovered in the earlier work where only the light-dark re-reduction (the actual rate), but not the pulse-dark re-reduction (PQH_2 saturated kinetics), was monitored. In severely limiting light only a rudimentary light–dark transient in the 820 nm signal can be recorded, because the high-potential donors are mostly reduced and PQ is oxidised.

The down-regulation of Cyt b_6f maximum turnover rate in low light indicates the presence of relatively high flux resistance in the carbon reduction cycle. Assimilatory power $F_A=[ATP^{4-}]/\{[ADP^{3-}][P_i^{2-}]\}\cdot\{[NADPH]/[NADP^+]\}$ has been used to characterise the driving force of photosynthesis [34]. Measurements have conclusively shown that if sufficient time is given for the enzymes of the carbon reduction cycle to adjust their activation state (>5 min), then high F_A is generated at limiting PFDs and it gradually decreases as photosynthesis approaches light saturation [35]. In our measurements, enzyme inactivation at the low PFDs of 73, 35 and 13 μmol quanta m^{-2} s^{-1} was evident from the following dark–light transient, where CO_2 uptake rate slowly increased and P700DW indicated strong ferredoxin signal (not shown). The absence of the low-light down-regulation of Cyt b_6f under low O_2 concentrations (Fig. 7) suggests that an oxygen-related mechanism generates the regulatory H^+ backpressure, e.g. by drainage

of reducing equivalents to O_2 photoreduction [20,36,37] or to consumption in mitochondria [38]. Alternatively, a redox-dependent control system may be involved in the low-light down-regulation of Cyt b_6f [39] (see below).

4.4. Cyclic e^- transport around PSI

The magnitude and physiological role of cyclic e^- transport around PSI has been an enigma for decades. Its measurement in intact leaves is complicated because no direct indicator of PSI e^- transport rate has been available as Chl fluorescence is for PSII. Thanks to available deconvolution methods for the optical signal in the 518–555 nm region, the post-illumination decay rate of electrochromic shift and re-reduction rate of Cyt *f* have been normalized on a per e^- basis, allowing the quantification of the e^- and H^+ transfer rates through Cyt b_6f that existed immediately prior to darkening [40] (the DIRK method, [32]). By comparing the e^- transport rate through Cyt b_6f with PSII e^- transport rate determined from Chl fluorescence, a high rate of cyclic e^- transport was detected in dark-adapted intact spinach leaves during the first seconds of illumination [40]. The occurrence of high rates of PSI cyclic e^- transport during the dark–light induction of photosynthesis, along with the fast water–water cycle, has been reported also in rice leaves by quantifying the PSI e^- transport from the fraction of unoxidised, but pulse-oxidisable P700, measured at 820 nm [20] and in tobacco leaves at saturating light and CO_2 [50]. The calculation of the PSI e^- transport rate from the time constant for the post-illumination re-reduction transient of the 820 nm signal indicated a drastic increase in PSI rates at saturating PFDs where PSII rates plateaued [33], indicating fast cyclic e^- transport around PSI at high light especially at elevated temperatures. An observation that the pulse-oxidisable fraction of P700 increased in parallel with NPQ suggested a model in which the normally non-oxidisable P700 is associated with PSI located in non-appressed regions of thylakoids. Under stress conditions this fraction becomes active in cyclic e^- transport, generating the proton gradient necessary for NPQ [26]. Though the interpretation of 820 nm signals containing the components from PC^+ and $P700^+$ is problematic in several aspects (discussed in [11,26]), there is little doubt that cycling of e^- back to the PSI donors can occur at high rates when photosynthesis is severely limited by the lack of e^- acceptors at PSI, e.g. during the induction of carbon reduction enzyme activity, during drought, or at its low ambient CO_2 concentrations. Our observations with Rubisco-deficient transgenic tobacco are in line with these observations, as well as with the observations on the Rubisco-deficient rice [20], considering that low Rubisco activity is equivalent to restricted CO_2 supply.

In normally functioning leaves during steady-state photosynthesis we did not detect cyclic e^- transport at limiting PFDs (as long as there was a measurable postillumination transient). At saturating PFDs we detected cyclic e^- transport in some leaves (sunflower), but failed to detect it in others (wild-type tobacco, *S. virgaurea*) though in the latter plant the photosynthetic rate was as severely limited as in the transgenic tobacco, where the cycle was detected. A relatively slow cyclic rate was detected in the high light- and low light-grown sunflower (Fig. 4 and Table 1) and low light-grown *T. cordata* at saturating light intensities (Table 1). A cyclic rate of about 10–15% of the linear rate may be necessary to compensate for the ATP deficiency if the Q-cycle is operating [3], but if 14 H^+ instead of 12 are required per turn of the rotor of the chloroplast ATP synthase producing 3 ATP [41]. Average cyclic rates in non-transformed plants were generally slower than this (Table 1). This ATP deficiency should be constant over the whole light response curve requiring that cyclic e^- flow remain at a fixed proportion of the linear rate [3]. Since there was no cyclic e^- transport at limiting PFDs in any leaf where the measurement was possible, we conclude that PSI cyclic e^- transport is not required for additional ATP generation in photosynthesis. If ATP deficiency exists, it must be compensated for by O_2-dependent alternative e^- transport processes, mentioned above. The importance of O_2 is supported by the clear positive effect of this gas on photosynthesis in the absence of photorespiration at saturating CO_2 concentrations [42,43]. Our failure to detect cyclic e^- transport in many leaves is at variance with the suggested principle role of cyclic e^- transport as a process that corrects imbalances in ATP/NADPH stoichiometry accompanying linear e^- transport alone [44]. However, in the latter work PSI cyclic e^- transport was not measured, but assumed to be impaired as a result of a mutation. Rather we explain the detected variable rate of cyclic electron flow as a result of the variable rate of non-photosynthetic ATP-consuming processes in the chloroplast, such as protein synthesis, etc. We also emphasize that our measurements can detect only relatively fast cyclic e^- transport rates. Slow rates may be sufficient for regulatory lumen acidification.

4.5. Photosynthetic control and non-photochemical quenching

Non-photochemical quenching of PSII fluorescence, a non-linear indicator of lumenal pH [45], is not proportional to the down-regulation of Cyt b_6f, as reported earlier [9] and confirmed in Fig. 8. However, at light saturation there still is a rather systematic relationship between the two parameters, suggesting that both may be pH-controlled, but the p*K* for the Cyt b_6f down-regulation is higher than for NPQ. As a result, with increasing lumenal acidity (e.g. with light intensity), Cyt b_6f becomes down-regulated first. At higher acidity NPQ is still increasing while Cyt b_6f is already maximally down-regulated. The inter-relationship is not universal, but in plants with lower carbon assimilation capacity Cyt b_6f is regulated relatively faster compared with NPQ (low light-grown *S. virgaurea*).

Remarkably, the low-light down-regulation of Cyt b_6f was not accompanied by a commensurate change in NPQ, though the amplitude of the former could sometimes be similar to the high-light down-regulation. This suggests that either the two processes are controlled by pH in different compartments in the thylakoid or the low-light control of Cyt b_6f is not related to lumenal pH. Eq. (4) suggests a pH-independent possibility to control the e^- arrival rate at PSI by changing the number of Cyt b_6f active in e^- transport. Lateral redistribution of Cyt b_6f in thylakoid membranes in parallel with state transitions, possible in our experiments, has been reported [46]. Alternatively, dimer–monomer transformation [47] may turn Cyt b_6f complexes into the slow (monomeric) state [48]. A recent model proposes redox-regulation of Cyt b_6f, where the signal comes from PSI acceptor side e^- carriers, probably from a thioredoxin. The unusual pH sensitivity of the regulatory component suggests that prior to the development of a ΔpH, the regulatory component will be rather sensitive to reduction, placing a tight control on e^- transport [39]. It is possible that the thioredoxin-related mechanism somehow controls the number of active Cyt b_6f complexes (e.g. by lateral movement or monomerisation) at the low light, whilst ΔpH directly controls the rate of PQH_2 oxidation at Cyt b_6f at the high light. The first process is expected to be slower than the second. A two-phase regulation of the light–dark re-reduction of $P700^+$, a fast phase in the range of seconds and slow phase in minutes domain, has been observed [49].

Notations

k_{Iq}	PSI excitation rate constant
k_I, k_{Im}	PSI e^- arrival rate constants, steady-state and substrate-saturated
k_{Cm}	Cyt b_6f e^- transport rate constants
k_{IF}	Steady-state k_I due to PSII electrons, determined from Chl fluorescence
N_I	Area density of PSI
N_{II}	Area density of PSII

Acknowledgement

This work was supported by a Research Professor grant to A.L from Estonian Academy of Science and by Grant 5236 from Estonian Science Foundation. Transgenic tobaccos were gifts from R.S.B.S., Australian National University; we thank J. Andrews, M. Badger and D. Price.

References

[1] H.H. Stiehl, H.T. Witt, Quantitative treatment of the function of plastoquinone in photosynthesis, Z. Naturforsch. 246 (1969) 1588–1598.
[2] P.R. Rich, A critical examination of the supposed variable proton stoichiometry of the chloroplast cytochrome *b*/*f* complex, Biochim. Biophys. Acta 932 (1988) 33–42.
[3] C.A. Sacksteder, A. Kanazawa, M.E. Jacoby, D.M. Kramer, The proton to electron stoichiometry of steady-state photosynthesis in living plants: a proton-pumping Q cycle is continuously engaged, Proc. Natl. Acad. Sci. 97 (2000) 14283–14288.
[4] U. Siggel, The control of electron transport by two pH-sensitive sites, in: M. Avron (Ed.), Proceedings of the 3rd International Congress on Photosynthesis, Elsevier, Amsterdam, 1974, pp. 645–654.
[5] C. Foyer, R. Furbank, J. Harbinson, P. Horton, The mechanisms contributing to photosynthetic control of electron transport by carbon assimilation in leaves, Photosynth. Res. 25 (1990) 83–100.
[6] E. Weis, D. Lechtenberg, Fluorescence analysis during steady-state photosynthesis, Philos. Trans. R. Soc. Lond., B 323 (1989) 253–268.
[7] J. Harbinson, C.L. Hedley, The kinetics of P 700+ reduction in leaves: a novel in situ probe of thylakoid functioning, Plant, Cell Environ. 12 (1989) 357–369.
[8] A. Laisk, V. Oja, Range of the photosynthetic control of postillumination P700 reduction rate in sunflower leaves, Photosynth. Res. 39 (1994) 39–50.
[9] T. Ott, J. Clarke, K. Birks, G. Johnson, Regulation of the photosynthetic electron transport chain, Planta 209 (1999) 250–258.
[10] C. Klughammer, U. Schreiber, Analysis of light-induced absorbance changes in the near-infrared spectral region: I. Characterization of various components in isolated chloroplasts, Z. Naturforsch. 46c (1991) 233–244.
[11] B. Genty, J. Harbinson, Regulation of light utilization in photosynthetic electron transport, in: N.R. Baker (Ed.), Photosynthesis and the Environment, Kluwer Acad. Publ., The Netherlands, 1996, pp. 67–99.
[12] V. Oja, I. Bichele, K. Hüve, B. Rasulov, A. Laisk, Reductive titration of Photosystem I and differential extinction coefficient of $P700^+$ at 810–950 nm in leaves, Biochim. Biophys. Acta 1658 (2004) 225–234.
[13] V. Oja, H. Eichelmann, R.B. Peterson, B. Rasulov, A. Laisk, Decyphering the 820 nm signal: redox state of donor side and quantum yield of Photosystem I in leaves, Photosynth. Res. 78 (2003) 1–15.
[14] A. Laisk, V. Oja, B. Rasulov, H. Rämma, H. Eichelmann, I. Kasparova, H. Pettai, E. Padu, E. Vapaavuori, A computer-operated routine of gas exchange and optical measurements to diagnose photosynthetic apparatus in leaves, Plant, Cell Environ. 25 (2002) 923–943.
[15] G.D. Price, J.W. Yu, S.v. Caemmerer, J.R. Evans, W.S. Chow, J.M. Anderson, V. Hurry, M.R. Badger, Chloroplast cytochrome b_6/f and ATP synthase complexes in tobacco: transformation with antisense RNA against nuclearencoded transcripts for the Rieske FeS and ATPs polypeptides, Aust. J. Plant Physiol. 22 (1995) 285–297.
[16] G.S. Hudson, J.R. Evans, S. Caemmerer von, Y.B.C. Arvidsson, T.J. Andrews, Reduction of ribulose-1,5-bisphosphate carboxylase/oxygenase content by antisense RNA reduces photosynthesis in transgenic tobacco plants, Plant Physiol. 98 (1992) 294–302.
[17] H. Eichelmann, V. Oja, B. Rasulov, E. Padu, I. Bichele, H. Pettai, P. Mänd, O. Kull, A. Laisk, Adjustment of leaf photosynthesis to shade in natural canopy: reallocation of nitrogen, Plant, Cell Environ. (in press).
[18] A. Laisk, V. Oja, Dynamic Gas Exchange of Leaf Photosynthesis. Measurement and Interpretation, CSIRO Publishing, Canberra, 1998.
[19] H. Eichelmann, A. Laisk, Cooperation of Photosystems II and I in leaves as analysed by simultaneous measurements of chlorophyll fluorescence and transmittance at 800 nm, Plant Cell Physiol. 41 (2000) 138–147.
[20] A. Makino, C. Miyake, A. Yokota, Physiological functions of the water–water cycle (Mehler reaction) and the cyclic electron flow around PSI in rice leaves, Plant Cell Physiol. 43 (2002) 1017–1026.
[21] R. Peterson, V. Oja, A. Laisk, Chlorophyll fluorescence at 680 and 730 nm and its relationship to photosynthesis, Photosynth. Res. 70 (2001) 185–196.
[22] B. Genty, J.M. Briantais, N.R. Baker, The relationship between quantum yield of photosynthetic electron transport and quenching of chlorophyll fluorescence, Biochem. Biophys. Acta 990 (1989) 87–92.
[23] W. Bilger, O. Björkman, Role of the Xanthophyll cycle in photoprotection elucidated by measurements of light-induced absorbance

changes, fluorescence and photosynthesis in leaves of *Hedera canariensis*, Photosynth. Res. 25 (1990) 173–185.
[24] A. Laisk, V. Oja, B. Rasulov, H. Eichelmann, A. Sumberg, Quantum yields and rate constants of photochemical and nonphotochemical excitation quenching, Experiment and model, Plant Physiol. 115 (1997) 803–815.
[25] V. Oja, A. Laisk, Oxygen yield from single turnover flashes in leaves: non-photochemical excitation quenching and the number of active PSII, Biochim. Biophys. Acta 1460 (2000) 291–301.
[26] A.J. Golding, G.N. Johnson, Down-regulation of linear and activation of cyclic electron transport during drought, Planta 218 (2003) 107–114.
[27] J. Lavergne, J.-P. Bouchaud, P. Joliot, Plastoquinone compartmentation in chloroplasts: II. Theoretical aspects, Biochim. Biophys. Acta 1101 (1992) 13–22.
[28] H. Kirchhoff, S. Horstmann, E. Weis, Control of the photosynthetic electron transport by PQ diffusion microdomains in thylakoids of higher plants, Biochim. Biophys. Acta 1459 (2000) 148–168.
[29] I.G. Tremmel, H. Kirchhoff, E. Weis, G.D. Farquhar, Dependence of plastoquinol diffusion on the shape, size, and density of integral thylakoid proteins, Biochim. Biophys. Acta 1607 (2003) 97–109.
[30] W.S. Chow, A.B. Hope, Kinetics of reactions around the cytochrome *bf* complex studied in intact leaf disks, Photosynth. Res. 81 (2004) 153–163.
[31] F. Drepper, M. Hippler, W. Nitschke, W. Haehnel, Binding dynamics and electron transfer between plastocyanin and Photosystem I, Biochemistry 35 (1996) 1282–1295.
[32] C.A. Sacksteder, D.M. Kramer, Dark-interval relaxation kinetics (DIRK) of absorbance changes as a quantitative probe of steady-state electron transfer, Photosynth. Res. 66 (2000) 145–158.
[33] J.E. Clarke, G.N. Johnson, In vivo temperature dependence of cyclic and pseudocyclic electron transport in barley, Planta 212 (2001) 808–816.
[34] U. Heber, S. Neimanis, K.J. Dietz, J. Viil, Assimilatory power as a driving force in photosynthesis, Biochem. Biophys. Acta 852 (1986) 144–155.
[35] U. Gerst, G. Schönknecht, U. Heber, ATP and NADPH as the driving force of carbon reduction in leaves in relation to thylakoid ennergization by light, Planta 193 (1994) 421–429.
[36] C. Wiese, L. Shi, U. Heber, Oxygen reduction in the Mehler reaction is insufficient to protect Photosystems 1 and 2 of leaves against photoinactivation, Physiol. Plant. 102 (1998) 437–446.
[37] K. Asada, The water–water cycle as alternative photon and electron sinks, Philos. Trans. R. Soc. Lond., B 355 (2000) 1419–1431.
[38] S. Krömer, H.W. Heldt, Respiration of pea leaf mitochondria and redox transfer between the mitochondrial and extramitochondrial compartment, Biochim. Biophys. Acta 1057 (1991) 42–50.
[39] G. Johnson, Thiol regulation of the thylakoid electron transport chain—a missing link in the regulation of photosynthesis, Biochemistry 42 (2003) 3040–3044.
[40] P. Joliot, A. Joliot, Cyclic electron transfer in plant leaf, Proc. Natl. Acad. Sci. 99 (2002) 10209–10214.
[41] H. Seelert, A. Poetsch, N.A. Dencher, A. Engel, H. Stahlberg, D.J. Müller, Proton powered turbine of a plant motor, Nature 405 (2000) 418–419.
[42] J. Viil, A. Laisk, V. Oja, T. Pärnik, Positive influence of oxygen on photosynthesis, Dokl. Akad. Nauk Ukr. SSR (Reports of the Acad. Sci. of the USSR) 204 (1972) 1269–1271.
[43] J. Viil, A. Laisk, V. Oja, T. Pärnik, Enhancement of photosynthesis caused by oxygen under saturating irradiance and high CO_2 concentrations, Photosynthetica 11 (1977) 251–259.
[44] Y. Munekage, M. Hashimoto, C. Miyake, K.-I. Tomizawa, T. Endo, M. Tasaka, T. Shikanai, Cyclic electron flow around Photosystem I is essential for photosynthesis, Nature 429 (2004) 579–582.
[45] G. Noctor, P. Horton, Uncoupler titration of energy-dependent chlorophyll fluorescence quenching and Photosystem II photochemical yield in intact pea chloroplasts, Biochim. Biophys. Acta 1016 (1990) 228–234.
[46] O. Vallon, L. Bulte, P. Dainese, J. Olive, R. Bassi, F.-A. Wollman, Lateral redistribution of cytochrome *b6/f* complexes along thylakoid membranes upon state transitions, Proc. Natl. Acad. Sci. U. S. A. 88 (1991) 8262–8266.
[47] W.A. Cramer, G.M. Soriano, M. Ponomarev, D. Huang, H. Zhang, S.E. Martinez, J.L. Smith, Some new structural aspects and old controversies concerning the cytochrome b_6f complex of oxygenic photosynthesis, Annu. Rev. Plant Physiol. Plant Mol. Biol. 47 (1996) 477–508.
[48] S. Heimann, C. Klughammer, U. Schreiber, Two distinct states of the thylakoid bf complex, FEBS Lett. 426 (1998) 126–130.
[49] A. Laisk, V. Oja, Coregulation of electron transport through PS I by Cyt b_6f, excitation capture by P700 and acceptor side reduction. Time kinetics and electron transport requirement, Photosynth. Res. 45 (1995) 11–19.
[50] C. Miyake, Y. Shinzaki, M. Miyata, K. Tomizawa, Enhancement of cyclic electron flow around PSI at high light and its contribution to the induction of non-photochemical quenching of Chl fluorescence in intact leaves of tobacco plants, Plant Cell Physiol. 45 (2004) 1426–1433.